Numerical models of diffusion and rainout of stratospheric radioactive materials

By B. DAVIDSON,[1] J. P. FRIEND and H. SEITZ, *Isotopes, Inc., Westwood, New Jersey*

(Manuscript received November 11, 1965)

ABSTRACT

A numerical model in two dimensions capable of simulating diffusion, transport, particle fall velocity and tropospheric rainout is described. The model incorporates a general anisotropic diffusion process. Rainout is simulated by fractional removal of debris at selected rain "formation" levels; the fraction removed at any latitude is proportional to the observed rainfall at that latitude. In the present paper the transport terms are neglected and an attempt is made to reproduce available data with a diffusion—rainout—settling velocity model.

The parameters of the model are varied in an attempt to reproduce quantitatively the known behavior of tungsten-185 injections in equatorial regions and, at least qualitatively, the behavior of high latitude stratospheric injections. Three types of models are described; they are characterized respectively by the principal diffusion axis being (*a*) along a horizontal surface, (*b*) along surfaces of constant potential temperature, and (*c*) along surfaces of constant potential vorticity. All three types can reproduce the latitudinal variation of rainout in a satisfactory manner, but only the third can reproduce the observed pattern of concentration in the stratosphere. The third type yields satisfactory results using lines of constant potential vorticity (only tentatively established by Hering and Borden) or using lines parallel to the tropopause as the principal axis of diffusion.

1. Introduction

The injection of a unique radioactive tracer (tungsten-185) into the lower tropical stratosphere by the U.S. test series (Hardtack) during the summer of 1958 and the associated stratospheric sampling program by high altitude aircraft during the succeeding two years constitute an extremely important experiment which can provide considerable understanding of the large-scale mixing and transport processes in the lower stratosphere. The observational data available from this experiment as summarized by FRIEND, FEELY, KREY, SPAR & WALTON (1961) are sufficiently detailed to challenge our previous notions concerning atmospheric transport and mixing processes in the lower stratosphere. The purpose of the present paper is to summarize a large number of numerical experiments which attempt to meet that challenge.

The injection of tungsten-185 was associated with a series of weapon tests which took place at 11.7° N from May to August, 1958. The stratospheric injection of tungsten-185 was estimated by FRIEND *et al.* (1961) at approximately 54 to 87.5 megacuries (corrected for decay to August 15, 1958). The average center of gravity of the injections is not accurately known, but it is assumed to lie within a ten thousand foot layer of the lower tropical stratosphere. The observed tungsten-185 distribution (two month mean) in the lower stratosphere, one year after the average injection time, is shown in Figure 1 (*a*). The heavy line indicates the analyst's impression of the distribution with latitude of the height of maximum concentration. The striking features of the concentration distribution are (*a*) the poleward declination of the axis of maximum concentration, (*b*) the maintenance of a center of maximum concentration slightly south of the original injection, (*c*) the development of a secondary maximum in north and in south polar regions, and (*d*) the large concentration gradient in the vertical just above the tropical tropopause. FEELY & SPAR (1960), BOLIN (1964), HERING & BORDEN (1964) and other authors have called attention to these features of the stratospheric

[1] Dr. B. Davidson is Director of the Geophysical Sciences Laboratory and Professor of Meteorology, New York University.

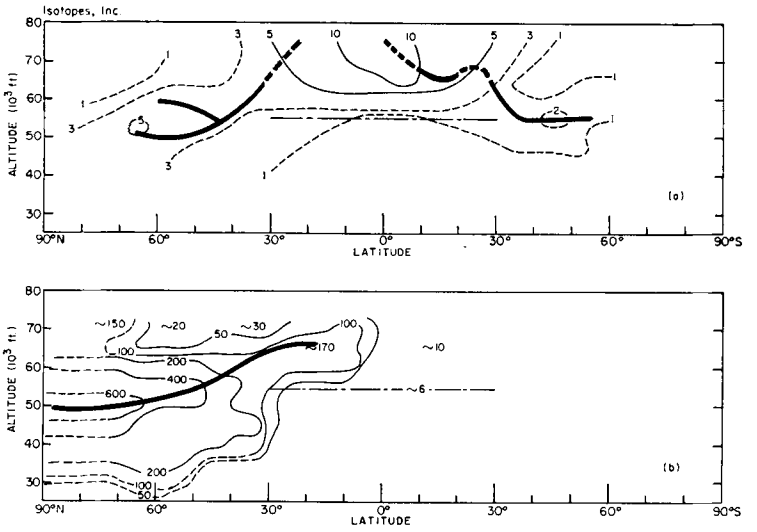

FIG. 1. (*a*) Mean May–June, 1959 distribution of tungsten-185 (dpm/SCF, corrected to 15 August 1958). (*b*) Mean January–April, 1962 distribution of strontium-90 (dpm/1000 SCF) from Soviet tests.

distribution and pointed out similarities between the artificially produced radionuclide and ozone distributions in the lower stratosphere.

Experimentation with the numerical diffusion model was designed to investigate systematically the consequences of a general mixing model. The objective is to isolate the simplest model structure which yields reasonable agreement with the observed features of the tungsten experiment. The relevant features are considered to be as follows:

(1) the distribution of concentration isopleths in the stratosphere,
(2) the decrease of central (maximum) concentration with time, and
(3) the observed meridional distribution of the combined rainout and dry fallout of the tungsten-185 for the first year after injection.

To test its general applicability, the model is further required to reproduce the gross features of an injection in the lower polar stratosphere. The 1961 Soviet test series approximates this type of injection. Figure 1 (*b*) shows the stratospheric distribution of strontium-90 resulting from this test series, six months after a mean injection time (FRIEND, FEELY & LEO, 1962). Due to the presence of strontium-90 from previous tests, it was necessary to use isotopic ratio (Sr-89/Sr-90) dating to identify the newly injected strontium-90. This process of identifying Soviet debris was feasible only up to May, 1962, at which time the U.S. introduced fresh debris into the stratosphere. The poleward slope of the axis of maximum concentration indicated in the Soviet data closely approximates that of the tungsten-185 data as shown in Figure 1 (*a*).

2. Numerical model

It is our intent to examine the possibilities of reproducing the main features of the observed data by means of eddy diffusion, particle settling and dry and wet fallout. In the absence of general circulation terms, the two-dimensional anisotropic diffusion equation incorporating the effects of particle fall velocity and variable density is, with good approximation for our domain of interest,

$$\varrho\frac{\partial q}{\partial t} = -\frac{\partial}{\partial r}(\varrho\Omega q) + \frac{\partial}{\partial r}\left(\varrho K_{rr}\frac{\partial q}{\partial r}\right) + \frac{1}{r^2\cos\phi}\frac{\partial}{\partial\phi}\left(\varrho\cos\phi K_{\phi\phi}\frac{\partial q}{\partial\phi}\right) + \frac{1}{r}\frac{\partial}{\partial r}\left(\varrho K_{r\phi}\frac{\partial q}{\partial\phi}\right) + \frac{1}{r\cos\phi}\frac{\partial}{\partial\phi}\left(\varrho\cos\phi K_{\phi r}\frac{\partial q}{\partial r}\right), \quad (1)$$

where:

ϱ = air density (gm/cm³); assumed to be a function of r only,
q = mixing ratio of radioactive material (gm/gm of air or dpm/gm of air),
K = coefficient of eddy diffusion (cm²/sec),
Ω = particle fall velocity (cm/sec),
ϕ = latitude (deg),
r = radial distance outward from the center of the earth (cm), and
t = time (sec).

It is to be noted that a term, $(r^2/r)\varrho K_{rr}(\partial q/\partial r)$, has been omitted from the right hand side of (1). Since the magnitude of r is of the order of 6×10^8 cm, this term is small with respect to the others and can be neglected.

It is not possible to solve this equation analytically for a complex atmosphere in which the density is a function of altitude and the coefficients of eddy diffusion may be functions of altitude, latitude and time. Furthermore, there is no simple way in which rainout can be incorporated into the equation. The method of finite difference solutions of parabolic differential equations with complex boundary and initial conditions is particularly appropriate for application to the problem considered in this paper. In what follows, the basis and principal features of the numerical model are presented.

If the tensor defined by the diffusion coefficients in (1) is assumed symmetric, i.e., $K_{\phi r} = K_{r\phi}$, then there exists a set of principal axes along which the off-diagonal or mixed derivative terms vanish. In what follows, we assume:

1. The local principal axis of diffusion is known at each point in the numerical grid.

2. The principal diffusion coefficients, K'_{11} and K'_{22}, are known at each grid point.

3. For the domain of interest, the r, ϕ coordinate system is sufficiently close to being cartesian to warrant the following transformations:

$$K_{\phi\phi} = \cos^2\alpha K'_{11} + \sin^2\alpha K'_{22}, \tag{2}$$

$$K_{rr} = \sin^2\alpha K'_{11} + \cos^2\alpha K'_{22}, \tag{3}$$

$$K_{r\phi} = K_{\phi r} = \cos\alpha \sin\alpha K'_{11} - \sin\alpha \cos\alpha K'_{22}, \tag{4}$$

where α is the angle between the $rd\phi$ direction (positive toward the north pole) and the direction of the principal diffusion axis. The absolute value of α is reasonably taken to be small; thus K'_{11} and K'_{22} represent quasi-horizontal and quasi-vertical diffusion coefficients respectively.

For numerical computations, it is convenient to express (1) in a μ, z coordinate system, where $\mu = \sin\phi$, $z = r - r_0$ and r_0 = the mean equatorial radius of the earth. Thus

$$\varrho\frac{\partial q}{\partial t} = -\frac{\partial}{\partial z}(\varrho\Omega q) + \frac{\partial}{\partial z}\left(\varrho K_{zz}\frac{\partial q}{\partial z}\right) + \frac{\partial}{r_0\partial\mu}\left([1-\mu^2]\varrho K_{\phi\phi}\frac{\partial q}{r_0\partial\mu}\right) + \frac{\partial}{\partial z}\left(\varrho\cos\phi K_{z\phi}\frac{\partial q}{r_0\partial\mu}\right) + \frac{\partial}{r_0\partial\mu}\left(\varrho\cos\phi K_{\phi z}\frac{\partial q}{\partial z}\right). \tag{5}$$

The numerical method involves considering an earth-atmosphere meridional plane as a grid of discrete points. For the models presented here the grid consists of 840 points; 30 along the μ-axis and 28 along the z-, or height axis. The grid interval in the vertical is a constant 1.5 km while it is variable in the μ-direction so that there are 17 grid points in the Northern Hemisphere and 12 grid points in the Southern Hemisphere.

An implicit, alternating direction scheme is used to integrate (5) numerically because of its inherent stability in producing convergent solutions and for numerical convenience. The finite difference analogue of (5) is expressed by (6) and (7) which are applied alternately with successive time increments.

$$\frac{q^{n+1}-q^n}{\delta t} = -\frac{1}{\varrho}\left[\frac{\delta}{\delta z}(\varrho\Omega q)\right]^n + \frac{1}{2\varrho}\left[\frac{\delta}{\delta z}\left(\varrho K_{zz}\frac{\delta q}{\delta z}\right)\right]^n + \frac{1}{2\varrho}\left[\frac{\delta}{\delta z}\left(\varrho K_{zz}\frac{\delta q}{\delta z}\right)\right]^{n+1} + \left[\frac{\delta}{r_0\delta\mu}\left((1-\mu^2)K_{\phi\phi}\frac{\delta q}{r_0\delta\mu}\right)\right]^n + \frac{1}{\varrho}\left[\frac{\delta}{\delta z}\left(\varrho\cos\phi K_{z\phi}\frac{\delta q}{r_0\delta\mu}\right)\right]^n + \left[\frac{\delta}{r_0\delta\mu}\left(\cos\phi K_{\phi z}\frac{\delta q}{\delta z}\right)\right]^n; \tag{6}$$

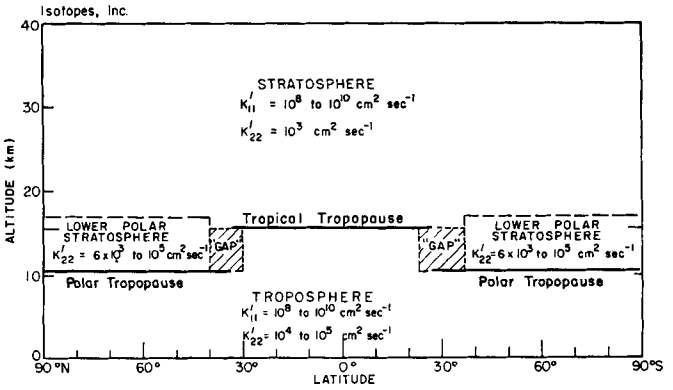

FIG. 2. Schematic representation of the distribution of diffusion coefficients characterizing the regions of the atmosphere in the numerical model.

$$\frac{q^{n+1}-q^n}{\delta t} = -\frac{1}{\varrho}\left[\frac{\delta}{\delta z}(\varrho\Omega q)\right]^n + \frac{1}{\varrho}\left[\frac{\delta}{\delta z}\left(\varrho K_{zz}\frac{\delta q}{\delta z}\right)\right]^n + \frac{1}{2}\left[\frac{\delta}{r_0\delta\mu}\left((1-\mu^2)K_{\phi\phi}\frac{\delta q}{r_0\delta\mu}\right)\right]^{n+1} + \frac{1}{2}\left[\frac{\delta}{r_0\delta\mu}\left((1-\mu^2)K_{\phi\phi}\frac{\delta q}{r_0\delta\mu}\right)\right]^n + \frac{1}{\varrho}\left[\frac{\delta}{\delta z}\left(\varrho\cos\phi K_{z\phi}\frac{\delta q}{r_0\delta\mu}\right)\right]^n + \left[\frac{\delta}{r_0\delta\mu}\left(\cos\phi K_{\phi z}\frac{\delta q}{\delta z}\right)\right]^n. \quad (7)$$

The superscripts in equations (6) and (7) above indicate values of the quantities at time n and time $n+1$. The alternating direction scheme is applied to only the second and third terms on the right in (5). It is apparent that, with respect to these terms, (6) is implicit in the z-direction and explicit in the μ-direction while (7) is implicit in the μ-direction and explicit in the z-direction; hence the term, "alternating direction". All other terms on the right are explicit. Centered differences are used to approximate all derivatives except for the first term which is evaluated as a backward difference since the fall velocity is always negative. The method of solution in two dimensions is described by DOUGLAS (1961). The only modification in our case is to adjust the boundary conditions so that the diffusive flux of material through the vertical and lateral boundaries of the system is always zero.

All models described in this paper incorporate a troposphere, tropopause, and stratosphere in a manner which is schematically illustrated in Figure 2. The vertical diffusion coefficient is assumed to be dependent on both stability (lapse rate) and vertical wind shear. Relatively large vertical diffusion coefficient values ($K'_{22} = 10^4$ to 10^5 cm² sec^{-1}) in the principal axis system are associated with the mean annual lapse rate of the troposphere, while, in general, relatively smaller (at least one order of magnitude) values of K'_{22} are associated with the stable inversions of the tropical stratosphere and upper polar stratosphere. Intermediate magnitudes of K'_{22} are associated with the isothermal layers of the lower polar stratosphere. The line of discontinuity between the large K'_{22} values of the troposphere and the smaller values of the stratosphere constitutes the tropopause.

In the models which are presented in detail, particle fall velocities (Ω) were determined as a function of altitude from calculations by JUNGE, CHAGNON & MANSON (1960) for spherical particles with 0.1 μ radius and 2 g/cm³ density. In the simulation of dry fallout, a value of $\Omega = 0.3$ cm/sec was used at the air-ground interface. This value was chosen to represent the effects of absorption, impaction and chemical and electrical affinities at the interface. The necessity in individual cases for a larger deposition velocity than is indicated by the terminal velocities of small particles has been shown from experiments by CHAMBERLAIN (1959, 1961) and CHAMBERLAIN & CHADWICK (1953).

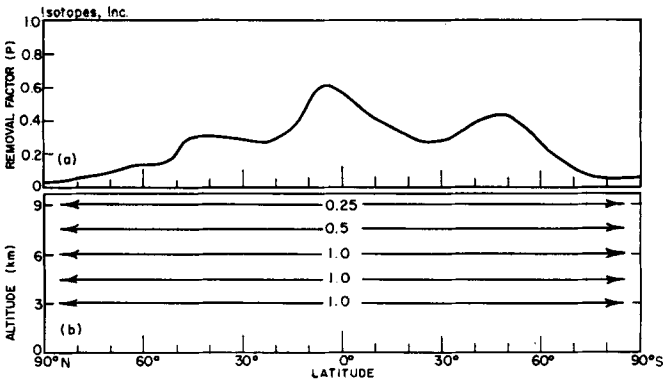

FIG. 3. Variation of the removal factor in the numerical model. (*a*) p as a function of latitude, (*b*) "a" values for the five removal levels.

In some models, the region between the polar and tropical tropopause is treated as a "gap" region and for these cases K'_{11} and/or K'_{22} are made relatively large as compared to their stratospheric values.

Wet fallout, i.e., removal by precipitation, is simulated in the models by the periodic removal of a fractional amount of q at a fixed grid point. This fractional amount removed (X) is a function of latitude and height and can be expressed:

$$X(\mu, z) = a(z)p(\mu)q(\mu, z), \qquad (8)$$

where $p(\mu)$ is a fraction proportional to the mean annual precipitation as given by MÖLLER (1951) and $a(z)$ is a height proportionality factor. The total amount removed in a fixed $\Delta\mu$ interval is

$$\Psi(\mu, t) = 2\pi r_0^2 \Delta\mu \int\int X(\mu, z)\varrho(z)\,dzdt. \qquad (9)$$

The removal levels and values of $p(\mu)$ and $a(z)$ are illustrated in Figure 3. In the models which are presented in detail, the fractional removal was accomplished every 5.0 days. A CDC 1604 computer was used for all computations with a time step of approximately 1.27 days.

In order to test the validity of the transformations (2) to (4), the finite difference approximation to (5), and the effect of the variable grid spacing ($\Delta\mu$) in the μ-direction in the Northern and Southern Hemispheres, a test model was run assuming the finite difference equivalent of a point source at $\mu = 0$ (the equator) and $z = 21$ km. The slope of the surface containing the principal diffusion axis was assumed constant and equal to 9.19×10^{-4}; $K'_{11} = 3 \times 10^9$ cm²/sec and $K'_{22} = 10^4$ cm²/sec were the values of the diffusion coefficients. The transformations (2) to (4) were used to obtain K_{rr}, $K_{r\phi}$ and $K_{\phi\phi}$. A measure of the adequacy of (2) to (5) is the degree to which the meridional slope of the level of maximum concentration, as determined from the computations, conforms to the assumed slope of the surface containing the principal diffusion axis. The extent of the agreement 6 months after injection is shown in Figure 4. The level of maximum concentration in a vertical section was estimated by parabolic interpolation of the computed concentrations at grid points bracketing the grid point at which a maximum appeared. The agreement is considered to be satisfactory and it is worth noting that the unequal grid intervals in the Northern and Southern Hemispheres do not seriously distort the results.

3. Tropical injection

For these experiments a vertical line source representing a tropical injection was assumed at $\mu = 0.2$ (11°32′ N) with a center of gravity ranging from 19.5 to 21 km according to the specific experiment. The results are reported for each of the following hypotheses:

1. The principal diffusion axis contained in horizontal planes, ($\alpha = 0$).
2. The principal diffusion axis contained in planes parallel to potential temperature surfaces in the stratosphere.

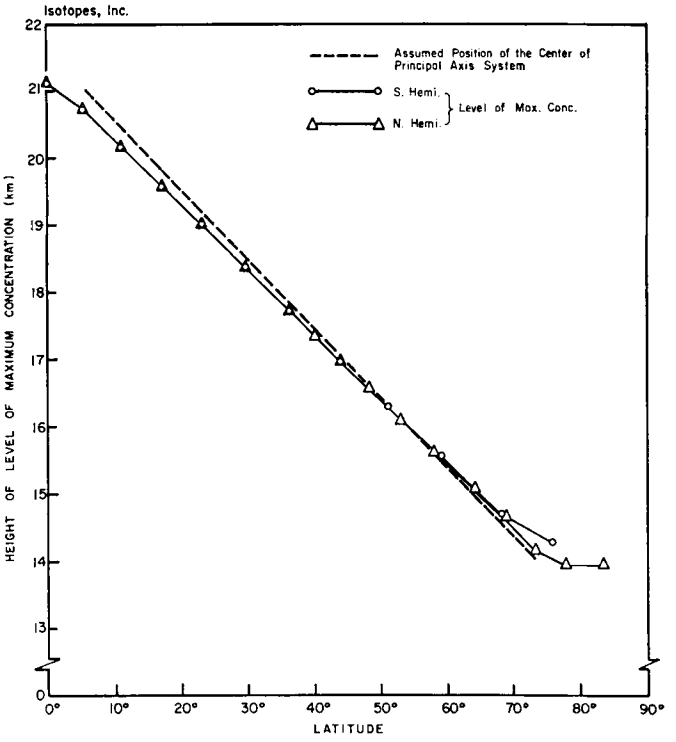

FIG. 4. Slope of the level of maximum concentration predicted by the numerical model six months after injection compared with the assumed slope of the principal diffusion axis.

3. The principal diffusion axis contained in planes parallel to the mean meridional configuration of the tropopause.

For hypothesis 1 the horizontal diffusion coefficient ($K'_{11} = K_{\phi\phi}$) varied from 10^9 to 10^{10} cm²/sec. The vertical diffusion coefficient ($K'_{22} = K_{zz}$) varied from 10^3 to 10^5 cm²/sec, i.e. 10^3 cm²/sec in the tropical stratosphere, 6×10^3 to 5×10^4 cm²/sec in the polar stratosphere, and 10^4 to 10^5 cm²/sec in the troposphere and "gap" regions. The horizontal diffusion coefficient was varied strongly with both latitude and height in attempts to obtain the observed meridional variation in the height of the maximum concentration. It was found possible to reproduce the desired stratospheric concentration patterns for only relatively small periods (1 to 4 months) after injection. Beyond these periods the altitude of maximum concentration tended to increase at a rate more rapid in mid and high latitudes than in equatorial regions. After times of 6 to 12 months the maximum concentrations exhibited distributions which were opposite in slope to the observed distribution, i.e., the altitude of maximum concentration had an upward instead of downward poleward slope. There are two main factors contributing to this undesirable behavior. The first is the effect of the vertical variation of air density. From (5) this effect can be isolated as

$$\frac{\partial q}{\partial t} = K_{zz} \frac{\partial q}{\partial z} \cdot \frac{\partial (\ln \varrho)}{\partial z} + \cdots . \qquad (10)$$

The sign of $(\partial/\partial z)(\ln \varrho)$ is always negative so that the sign of the contribution of the variable density term to $\partial q/\partial t$ is determined by the sign of $\partial q/\partial z$. For an isolated point source, therefore, the effect of the variable density term is to produce a positive $\partial q/\partial t$ above the source and a negative $\partial q/\partial t$ below. The magnitude of this effect is proportional to the magnitude of the vertical diffusion coefficient, K_{zz}. The second factor comes from the introduction of large vertical diffusion coefficients in the "gap" regions. These large coefficients were needed in order to duplicate the time rate and meri-

dional distribution of surface deposition. This meridional variation of the vertical diffusion coefficients in the lower stratosphere, coupled with the variable density factor and the tropospheric sink, caused the level of maximum concentration to rise more rapidly in mid latitudes than at the equator.

It was, therefore, concluded that, within the range of diffusion coefficients considered to be even remotely reasonable, it was impossible to reproduce correctly the meridional distributions of both the surface deposition and the stratospheric concentration on the basis of diffusion processes alone when the principal diffusion axis is assumed to be everywhere horizontal.

The consequences of hypothesis 2, namely that the principal diffusion axis parallels the isentropes, were examined despite the fact that the observed slope of the isentropes at 20 km is less than one half the observed slope of the level of maximum concentration of the tungsten-185 distribution. It was considered that suitable adjustments of K'_{11} and K'_{22} in such an inclined diffusion axis scheme might lead to better agreement than had been obtained with the horizontal axis.

The most elaborate experiment of this type involved varying the slopes of the isentropes seasonally, setting the vertical diffusion coefficient in the "gap" region proportional to the magnitude of the monthly mean jet and fixing the horizontal diffusion coefficients according to the vertical and meridional distribution of the vector standard deviation of the wind (extrapolating values into the stratosphere). Data for these seasonal and spatial variations were obtained from meridional cross-sections published by the U.S. Weather Bureau (1961). For this set of experiments, K'_{11} varied from 10^8 to 10^{10} cm^2/sec and K'_{22} varied from 10^3 to 10^5 cm^2/sec.

The results were not satisfactory. The large diffusion coefficients in the "gap" region and the strong tropospheric rainout mechanism made it impossible to maintain the desired slope of the level of maximum concentration in the stratosphere equatorward of the "gap" region, although more satisfactory results were obtained poleward of the "gap" region. The large spatial variation of the primed diffusion coefficients in the "gap" region tended to obscure the effect of the sloping principal diffusion axis. The one positive conclusion from this set of experiments was that the anisotropic model, with the principal axis of the diffusion tensor oriented along the isentropic surfaces, did significantly slow down the rate of rise of the level of the maximum concentration in the presence of a strong tropospheric sink and relatively large values of K'_{11} and K'_{22} in the "gap" regions.

Finally, hypothesis 3 was investigated by assuming that the quasi-horizontal principal diffusion axis in the stratosphere and upper troposphere is approximately parallel to the mean annual tropopause configuration at all levels in the meridional plane. The mean slope of the tropopause in the jet stream region was determined each month from meridional cross-sections for 1958, (U.S. Weather Bureau, 1961). These slopes were then averaged for the year and located at the mean annual latitudinal position of the jet core. The slope thus determined is about 4.1×10^{-3} and in the present model extends approximately from 33.5° to 46.5° N latitude. The principal diffusion axis was assumed parallel to this tropopause configuration from 6 km to 22.5 km; above 22.5 km the slopes were reduced to 2.9×10^{-3} mostly because the slopes of the lines of constant potential vorticity (HERING & BORDEN, 1964) decrease with altitude in the stratosphere. It is recognized that the method of averaging is somewhat arbitrary and must be considered in the interpretation of the results. This, however, is not considered to be a serious drawback in the present development of the model.

It was found for this last scheme that all of the observed features of the tungsten experiment could be reproduced with an extremely simple set of diffusion coefficients. A value of $K'_{11} = 4 \times 10^9$ cm^2/sec throughout the system; a value of $K'_{22} = 10^3$ cm^2/sec throughout the stratosphere and a value of $K'_{22} = 4 \times 10^4$ throughout the troposphere were sufficient to yield satisfactory results. In this series of experiments it was assumed that the injection took place at $\mu = 0.2$ (11°32′ N); at $z = 18$ km, $q = 11.3$ dpm/g of air and at $z = 19.5$ km, $q = 28.5$ dpm/g of air. This source configuration corresponds to a total injection of 70 megacuries, approximately the mid-point of the range of estimates of 54 to 87.5 megacuries.

In Figure 5, the decrease with time of central concentration predicted by the model is compared with the observed decrease. The meri-

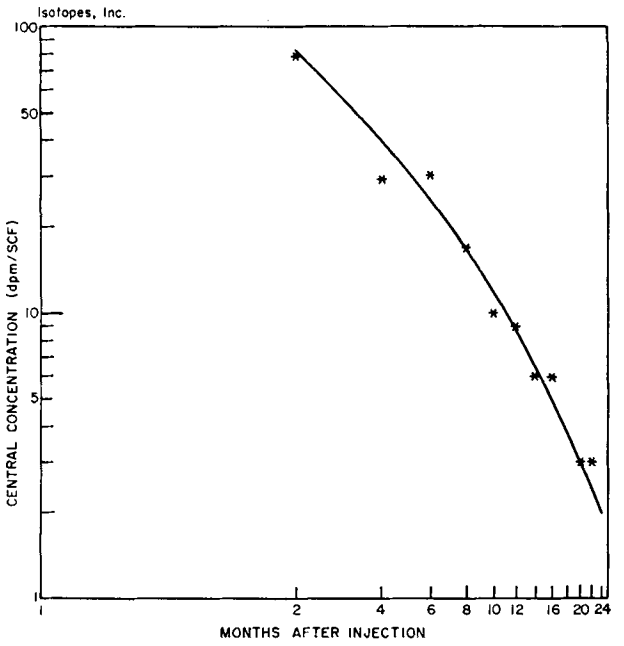

FIG. 5. Decrease of central concentration with time. Asterisks are plots of observed bi-monthly values of tungsten-185. Solid curve is prediction results of numerical model.

dional distributions of total deposition, one year after injection, as predicted by the model and as estimated from observed data (FRIEND *et al.*, 1961) are shown in Figure 6. The predicted peaks occurred at the same latitudes as observed in the Southern Hemisphere and the Tropics while the predicted Northern Hemisphere peak occurred about 5 degrees north of the observed peak. Also, the relative magnitudes of the predicted peaks corresponded well with the observed data. There was, however, some disparity between the totals of global fallout represented by the two curves. The model indicated 45 megacuries deposited while the observed estimate was 61 megacuries. This difference can be attributed to two factors—

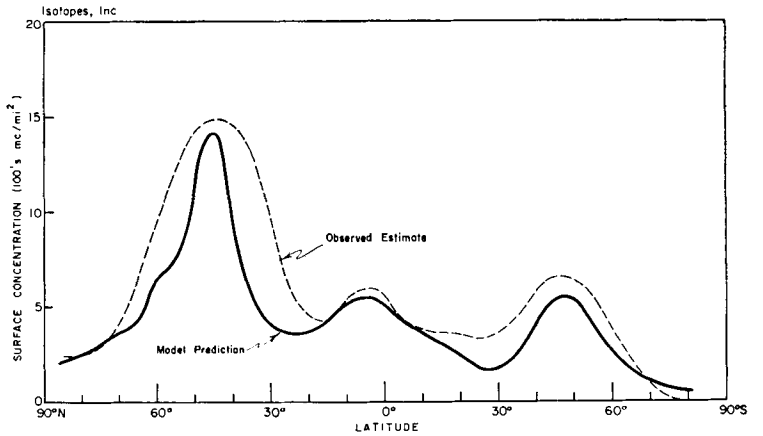

FIG. 6. Distributions of surface deposition of tungsten-185 one year after injection.

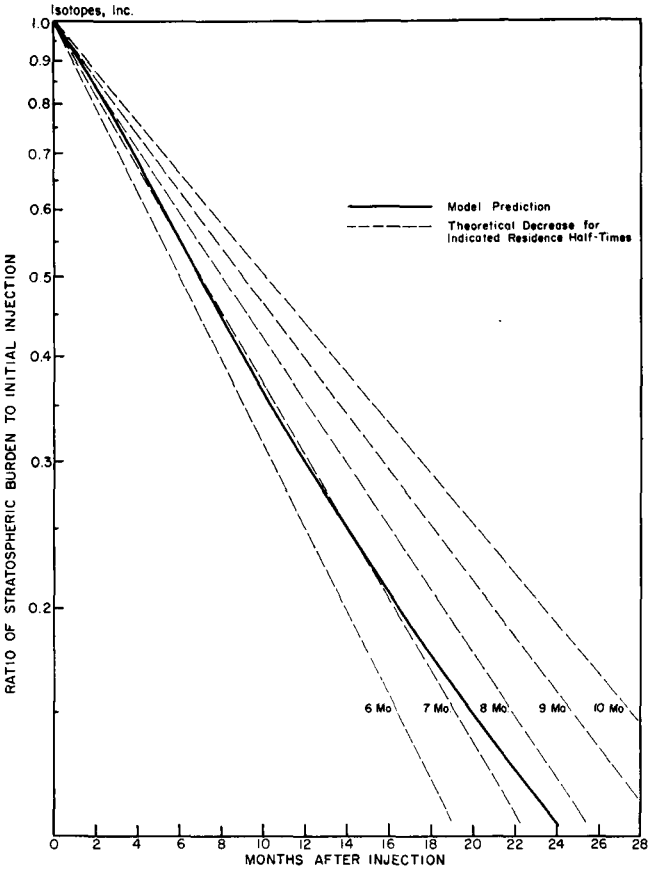

FIG. 7. Decrease of stratospheric burden with time predicted by numerical model for tropical injection.

the magnitude of the injection in the model was not large enough and/or the estimate of surface deposition from the observed data was too large. The experimental uncertainties in both of these factors are sufficient to account for the above mentioned disparity. The injection in the model could justifiably be accepted as 85 instead of 70 megacuries. Also, the estimate of total surface deposition by FRIEND *et al.* (1961) for 16 months after the tungsten injections is 77.5 megacuries (corrected to August 15, 1958) which exceeds by 10% the total amount initially put into the stratosphere in the model. Indicative of the uncertainty in the estimates of surface deposition is the comparison of HARDY's (1960) estimate of 50 megacuries for the 16 month period with the above 77.5 megacuries value.

Another disparity between the observed and model predicted distributions in Figure 6 is the difference in spread of the distributions about the Northern Hemisphere peak. Attempts to improve the spread of the predicted distribution by variations of the magnitudes of K'_{11} and K'_{22} in the troposphere were not successful. It is felt, however, that considerable improvement can be realized by a four season model in which there are a seasonal shift meridionally of the tropopause configuration and a seasonal variation in the magnitudes of the wet removal factors.

In view of the uncertainties of the observed surface distribution and magnitude of initial injection and of the simplicity of the model structure, these results are considered satisfactory.

Further satisfactory results were achieved by the model with respect to the stratospheric residence half-times for the material. The decrease with time of the stratospheric inventory

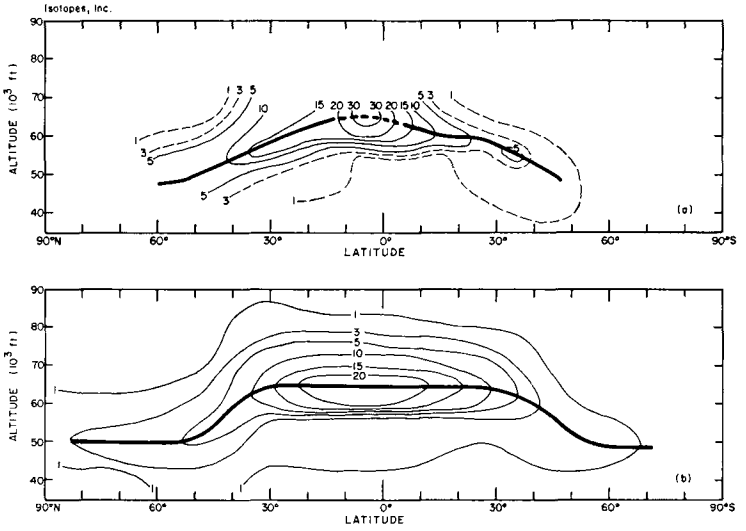

FIG. 8. Distributions of tungsten-185 six months after injection. (*a*) Observed mean for Nov.–Dec., 1958 (dpm/SCF corrected to 15 August 1958). (*b*) Prediction by numerical model (dpm/SCF).

in the model has been plotted in Figure 7 and compared to rates of decrease corresponding to various theoretical residence half-times. An average residence half-time of 7 months is indicated for the model during the first 16 months after injection. Thereafter, the residence half-time tends to increase to 9 and 10 months. These results are in accord with the 5 to 9 months estimates for stratospheric material made by FRIEND *et al.* (1961) based on the possible range of magnitudes of injection and stratospheric inventories estimated from observed data.

Figures 8, 9 and 10 compare the observed stratospheric distributions of tungsten with the model prediction 6, 12 and 24 months after injection, respectively. The gross features of the observed tungsten-185 distributions were satisfactorily reproduced by the numerical model at 6 and 12 months after injection but

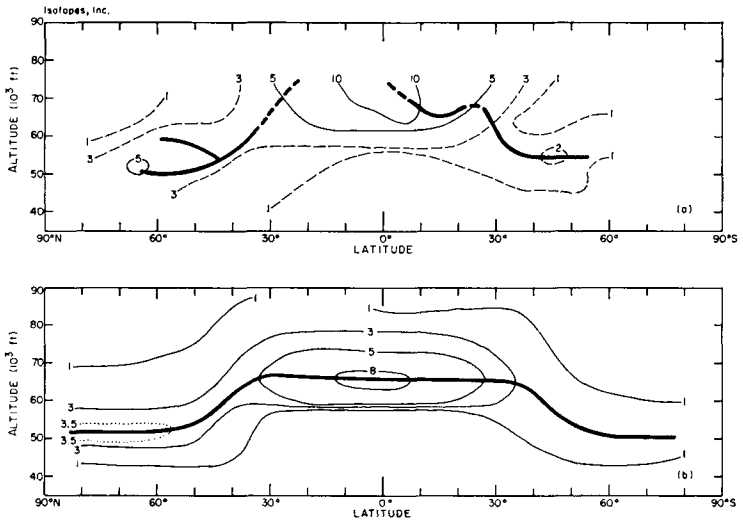

FIG. 9. Distributions of tungsten-185 twelve months after injection. (*a*) Observed mean for May–June, 1959 (dpm/SCF corrected to 15 August 1958). (*b*) Prediction by numerical model (dpm/SCF).

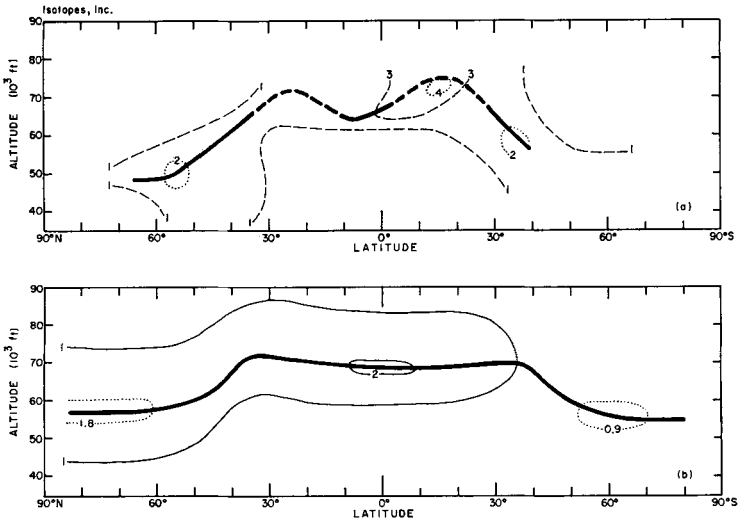

FIG. 10. Distributions of tungsten-185 twenty-four months after injection. (*a*) Observed mean for May-June, 1960 (dpm/SCF corrected to 15 August 1958). (*b*) Prediction by numerical model (dpm/SCF).

the similarity of features is noticeably less after 24 months. It must be borne in mind, however, that after 24 months, the observed data are much less reliable. The important gross features to be compared between the observed and model results are: (1) decrease in height of 15,000 feet of the level of maximum concentration from 20° to 60° latitude in both hemispheres; (2) strong vertical concentration gradient in the lower tropical stratosphere just above the tropical tropopause and a considerable decrease in this gradient poleward in the lower polar stratosphere; (3) the tendency for the tropical center of maximum concentration to move equatorward; and (4) development of secondary centers of maximum concentration at higher latitudes.

After 24 months significant difference in concentration distributions appeared, as shown in Figure 10. The observed data indicated a movement of the tropical center of maximum concentration well into the Southern Hemisphere whereas this center remains within the vicinity of the equator in the model. The observed data are considered quite suspect at this time. In the observed concentration distribution 22 months after injection there is no indication of movement of the center of maximum concentration into the Southern Hemisphere. Also, at high latitudes, the height of the level of maximum concentration rose to 57 thousand feet in the model, but remains at approximately 50 thousand feet in the observed data.

4. Polar injection

Since the possibility existed of fortuitous agreement between predicted and observed results for these experiments with tropical injections, it was decided to examine the consequences of the same hypothesis (i.e. the principal axis of diffusion parallels the tropopause configuration) as applied to a lower polar stratospheric injection. For this investigation the 1961 Soviet test series was selected as representative of such an injection.

The observed strontium-90 data for this test series were determined by isotopic ratio (Sr-89/Sr-90, Ce-144/Sr-90) dating because there was a considerable amount of strontium-90 in the atmosphere due to previous testing. Also, these data are not considered beyond April, 1962 because of the injection of new strontium-90 by U.S. tests after this date. Thus, the observed data are confined essentially to the winter months. The model was adapted for a winter season experiment by assuming the same average slope (4.1×10^{-3}) of the tropopause in the jet core region but the latitudinal position of the jet core was displaced some 15 degrees equatorward.

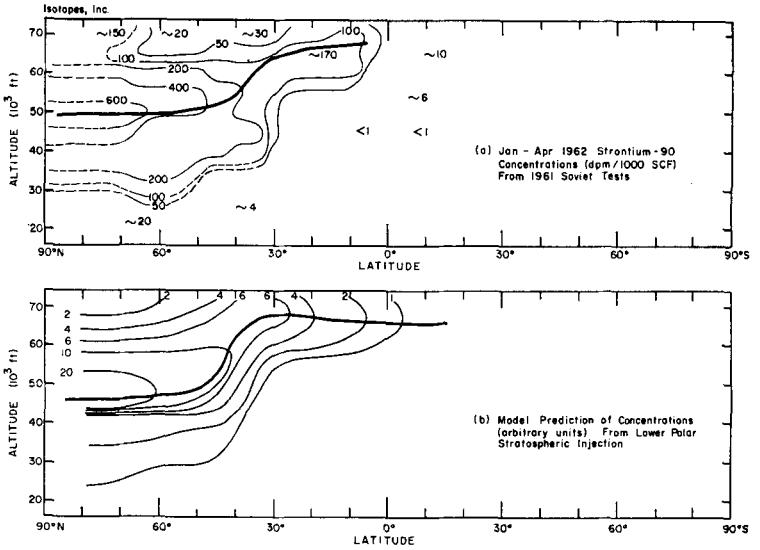

FIG. 11. Distribution of stratospheric concentration six months after polar stratospheric injection. (*a*) Observed estimate of 1961 Soviet debris. (*b*) Numerical model prediction.

It was fairly well known that the major testing in this series was conducted at Novaya Zemlya, approximately 75° N latitude, but the altitude, magnitudes and vertical distributions of the individual injections are highly speculative. In the model, therefore, the magnitude of the injection was arbitrary and, using the observed data as guide lines for altitude and vertical distribution, an equally distributed line source was put in between 45 and 50 thousand feet.

In general, the observed strontium-90 data from this test series do not constitute so reliable and unique an experiment as the tungsten-185 data.

At the time of the writing of this paper, sufficient experimentation with the polar injection had not been completed to permit full evaluation of the overall capability of the model. The results of early experiments in this series showed good agreement between the observed stratospheric distribution of strontium-90 ap-

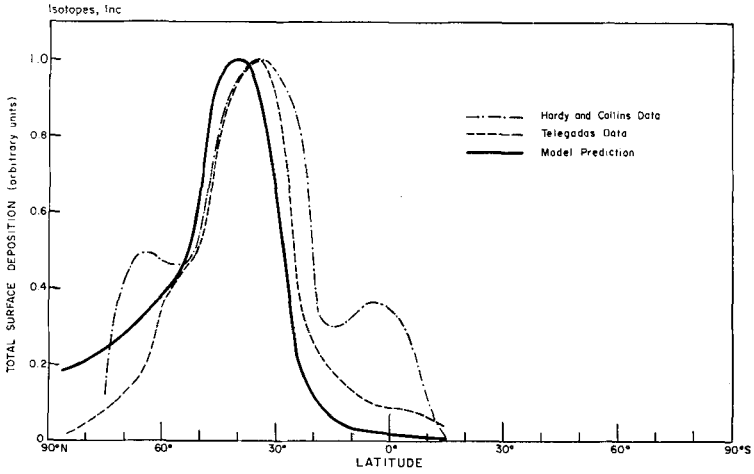

FIG. 12. Distribution of surface deposition six months after polar stratospheric injection.

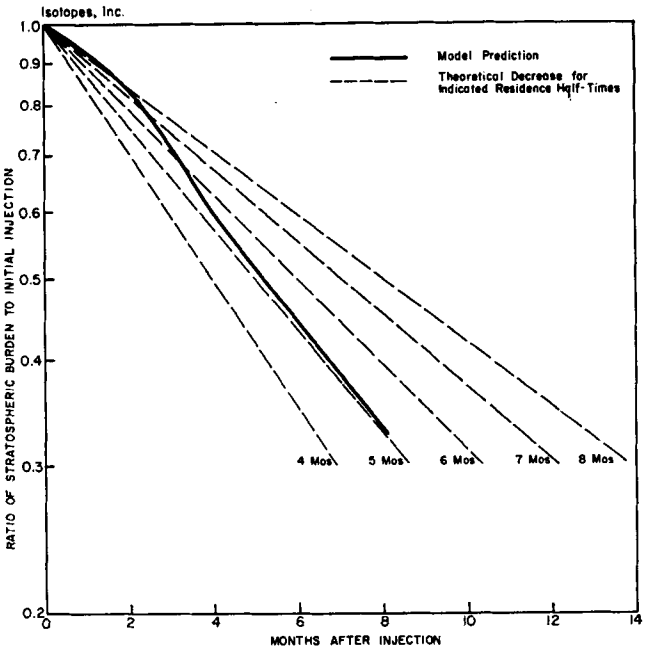

FIG. 13. Decrease of stratospheric burden with time as predicted by the numerical model for a polar injection.

proximately 6 months after injection and the distribution predicted by the model (Figure 11). The observed upward slope of the level of maximum concentration toward the equator was reproduced quite well by the model. Unfortunately sufficient observed data are not available to determine the rate of decrease of the central concentration during the period.

In Figure 12, the best model surface deposition result is compared with the estimate of distribution from HARDY & COLLINS (1962) and COLLINS (1963) and with an estimate determined from data by TELEGADAS (1963) which incorporates a correction for rainfall. The better agreement between the model prediction and the Telegadas estimate is noteworthy since the wet-fallout simulation in the model is based on the average meridional distribution of rainfall.

The observed data of the decrease with time of the stratospheric burden of Sr-90 from 1961 Soviet tests are insufficient to provide a worthwhile quantitative estimate of residence half-times of the material. It is generally recognized that the residence time of debris in the atmosphere is dependent upon the height, latitude and season of injection and that it is shorter for higher latitudes and lower altitudes (FRIEND *et al.*, 1961 and BOLIN, 1964). Residence half-times of 3 to 6 months have been considered reasonable for the lower polar stratosphere in computations of burden trends (FRIEND *et al.*, 1961). Figure 13 shows the decrease of stratospheric burden with time as predicted by the numerical model. A residence half-time of 5 to 7 months is indicated for the curve. These values are generally lower than those predicted in the tropical injection and are in reasonable accord with the investigators cited above.

The experimental results of the polar injection presented above required a winter season adaptation of the model as used for the tropical injection. This adaptation is considered realistic and it is felt that the incorporation of seasonal variation of meteorological parameters will produce a single model capable of satisfying both the tropical and polar injection prediction criteria.

5. Conclusion

A numerical model of eddy diffusion, particle settling and removal in the stratosphere-troposphere-earth's surface system has been devel-

oped which predicts satisfactorily the behavior of injections of material into the lower tropical stratosphere. Applying of this model to lower polar stratospheric injections lead to predictions which, at least, are not in gross error. The model has a relatively simple set of parameters for characterizing the transport-removal system. A prime feature of the model is that the local quasi-horizontal principal axis of the diffusion tensor lies in surfaces parallel to the tropopause. This is an empirical result of the present study.

It has been widely held that large-scale eddy diffusion is basically an isentropic process. The observation was made by FEELY & SPAR (1960) that the tungsten-185 distribution appeared to have been affected by non-isentropic motions. Since basically, the same data considered by them were used in this study, it is perhaps not surprising that a "non-isentropic" model yielded the best results. HERING & BORDEN (1964), in studying ozone transport, computed surfaces of equal potential vorticity in the stratosphere; they concluded that the ozone transport may occur in motions parallel to these surfaces which are more nearly parallel to the tropopause than are the isentropic surfaces. NEWELL (1964), in studying potential energy–kinetic energy relationships in the stratosphere, concluded that non-isentropic processes took place there, especially in mid-latitude regions. These findings, along with the current model study, indicate that the primary large-scale mixing processes in the lower stratosphere may take place along surfaces of constant potential vorticity. This statement must be qualified as conjectural, since there are no reliable climatological stratospheric potential vorticity data which could be used in proof. The numerical experiment embodied in the present study is, however, sensitive enough to show that some non-isentropic processes are involved in large-scale mixing motions of the lower stratosphere. Furthermore, it appears unnecessary to ascribe a dominant role to meridional circulations in the transport of material in that portion of the atmosphere.

6. Acknowledgements

The authors wish to extend special thanks to Dr. H. W. Feely, Isotopes, Inc., for his continuous assistance and helpful suggestions. To Dr. L. Machta, U.S. Weather Bureau, for his contributions to the rainout simulation techniques and his many comments during the course of this work, we also extend special thanks. We are grateful for the suggestions regarding difference techniques made by Mr. B. W. Ramsey, U.S. Weather Bureau, and Dr. N. Newman, New York University, and we wish to express our appreciation to Dr. L. Tick and Mr. S. Jaffee, New York University, for their contribution to the programming of the model. We sincerely thank Mrs. K. Robinson, Isotopes, Inc., for the drafting of all figures.

REFERENCES

BOLIN, B., 1964, The general circulation of the atmosphere as deduced with the aid of tracers. Agenda Item 3: Discussion of Meteorological Problems with WMO Experts, Thirteenth Session of UNSCEAR, New York, N.Y.

CHAMBERLAIN, A. C., 1959, Deposition of iodine-131 in northern England in October, 1957. *Quart. J. Roy. Meteor. Soc.*, **85**, 350.

CHAMBERLAIN, A. C., 1961, Aspects of the deposition of radioactive and other gases and particles. *Int. J. Air Poll.*, **3**.

CHAMBERLAIN, A. C., and CHADWICK, R. C., 1953, Deposition of airborne radioiodine vapour. *Nucleonics*, **2**, 22.

COLLINS, WM. R., 1963, Strontium-90 deposition on the earth's surface from 1958 through 1962. HASL-140, Fallout Program Quarterly Summary Report, Health and Safety Laboratory, AEC, New York, N.Y., pp. 240–247.

DOUGLAS, J., 1961, Numerical methods for parabolic equations, in *Advances in Computers*, **2**, New York, Academic Press.

FEELY, H. W., and SPAR, J., 1960, Tungsten-185 from nuclear bomb tests as a tracer for stratospheric meteorology. *Nature*, **188**, pp. 1062–1064.

FRIEND, J. P., FEELY, H. W., KREY, P. W., SPAR, J., and WALTON, A., 1961, The High Altitude Sampling Program. Final Report: DASA 1300, 3, Discussion of HASP Results; 4, The Application of HASP Data. Defense Atomic Support Agency, Contract No. DA-29-044-XZ-609. Isotopes, Inc., Westwood, New Jersey.

FRIEND, J. P., FEELY, H. W., and LEO, M. W. M., 1962, Project Stardust, 6th Quarterly Report, DASA 1306, Defense Atomic Support Agency Contract No. DA-49-146-XZ-079. Isotopes, Inc., Westwood, New Jersey.

HARDY, E. P., JR., 1960, Tungsten-185 deposition on the earth's surface. HASL-95, Fallout Program Quarterly Summary Report, Health and Safety Laboratory, AEC, New York, N.Y., pp. 203–207.

HARDY, E., and COLLINS, W., 1962, Strontium-90 deposition on the earth's surface from 1958 through 1961. HASL-131, Fallout Program

Quarterly Summary Report, Health and Safety Laboratory, AEC, New York, N.Y., pp. 221–229.

HERING, W. S., and BORDEN, T. R., JR., 1964, Analysis of the seasonal and synoptic-scale variations in the vertical ozone distribution. International Atmospheric Ozone Symposium, Albuquerque, New Mexico.

JUNGE, C. E., CHAGNON, C. W., and MANSON, J. E., 1960, Stratospheric Aerosols. AEC Contract AT (49-7)-1431, Geophysics Research Directorate, ARDC, Bedford, Mass., p. 69.

MÖLLER, F., 1951, Vierteljahrskarten des Niederschlags für die ganze Erde. *Peterm. Geogr. Mitt.*, 1, pp. 145–156.

NEWELL, R. E., 1964, Stratospheric energetics and mass transport. *Pure and Applied Geophysics*, 58, II, pp. 145–156.

TELEGADAS, K., 1963, Global Integrals of monthly Sr-90 fallout, January 1958–May, 1962. HASL-135, Fallout Program Quarterly Summary Report, Health and Safety Laboratory, AEC, New York, N.Y., pp. 215–239.

U.S. WEATHER BUREAU, 1961, Meridional cross-sections, upper winds over the Northern Hemisphere. Technical Paper No. 41, U.S. Dept. of Commerce, Washington, D.C.

ЧИСЛЕННЫЕ МОДЕЛИ ДИФФУЗИИ И ВЫМЫВАНИЯ РАДИОАКТИВНЫХ ОСТАТКОВ ДОЖДЕМ

Рассмотрена численная двухмерная модель, описывающая диффузию, перенос, скорость падения частиц и тропосферное вымывание радиоактивных остатков. Эта модель включает также общую анизотропную диффузию. Вымывание радиоактивных осадков имметируется частичным устранением их в выбранных уровнях «образования» дождя, причем величина этого изъятия каждой широты пропорциональна наблюдавшемуся выпадению. В настоящей статье пренебрегается членами, выражающими перенос, и делается попытка воспроизвести действительные данные с помощью диффузии–вымывания–скорости оседания.

Параметры модели менялись для того, чтобы воспроизвести качественно известное поведение инжекций вольфрама-185 в экваториальных областях и, по крайней мере, качественно поведение стратосферных инжекций в высоких широтах. Описаны три типа моделей, различающихся по расположению главного направления (оси) диффузии: а) вдоль горизонтальных поверхностей, б) вдоль поверхностей постоянной потенциальной температуры и в) вдоль поверхностей постоянного потенциального вихря. Все три модели удовлетворительно воспроизводят широтные изменения величины вымывания, но только третья описывает наблюдаемое распределение концентраций в стратосфере. Последняя модель дает удовлетворительные результаты как при использовании в качестве главного направления диффузии линий постоянного потенциала, установленных экспериментально (Hering и Border), так и линий параллельных тропопаузе.